ACS Catalysis

pubs.acs.org/acscatalysis
Research Article

High-Throughput Enabled Iridium-Catalyzed C−H Borylation Platform for Late-Stage Functionalization

Janis M. Zakis, Rebeka A. Lipina, Sharon Bell, Simon R. Williams, Maurus Mathis, Magnus J. Johansson, Joanna Wencel-Delord, and Tomas Smejkal*

Cite This: ACS Catal. 2025, 15, 3525−3534
Read Online

ACCESS | Metrics & More | Article Recommendations | Supporting Information

ABSTRACT: In this work, we present a dedicated, high-throughput reaction optimization platform allowing for the rapid evaluation of regiodivergent C−H borylation protocols while minimizing the amount of starting material required. The workflow was applied to a diverse set of fragment-like compounds, pharmaceuticals, and agrochemicals, and its practicality was demonstrated by successfully isolating 36 derivatives of bioactive compounds. Leveraging the informer library approach, we provide a comprehensive, side-by-side comparison of catalytic methods, revealing insights into the strengths, limitations, and versatility of each borylation protocol. Surprising reactivity patterns, effectiveness of ligand-free C−H borylation, and the utility of previously reported directed C−H borylation catalysts outside of their expected substrate scope have been noticed. This study highlights the potential of dedicated high-throughput optimization platforms to expand the practical utility of late-stage functionalization protocols for pharmaceutical and agrochemical research.

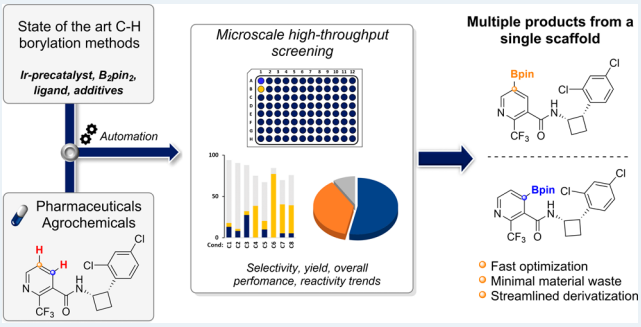

KEYWORDS: *high-throughput experimentation, late-stage functionalization, C−H borylation, miniaturization, informer library*

INTRODUCTION

High-throughput experimentation (HTE) has emerged as a transformative approach that may revolutionize how chemists explore the reaction space and optimize catalytic systems. This powerful methodology, which enables the parallel execution of multiple experiments and the simultaneous evaluation of numerous variables, is becoming an indispensable tool in both academic and industrial settings and dramatically reduces the time and resources required for reaction optimization.[1−8]

Late-stage functionalization (LSF) of C−H bonds represents an important strategy for accelerating the discovery, optimization, and development of novel bioactive molecules.[9−11] Direct installation of functional groups onto existing biologically active compounds allows for the rapid synthesis of related analogues,[12] preparation of putative oxidized metabolites,[13] and other biological probes.[14] Compared to the linear and time-consuming de novo synthesis, these short and divergent routes have a transformative potential for synthetic productivity. Despite the numerous recent publications on novel C−H LSF methodology, actual discovery programs still heavily rely on more traditional transformations of prefunctionalized building blocks.[15−17] A possible obstacle to the broader use of C−H LSF could be the immaturity of the field, where the development of better and more general methods is still required. However, we would argue that it is to a larger extent the perceived intellectual and experimental effort required to identify, test, and individually optimize each new substrate-methodology combination, particularly when combined with the limited material availability and tight timelines of a typical research program. Various strategies have been proposed to facilitate the selection of the most appropriate LSF method for a given substrate. These include the publication of both successful and unsuccessful substrate scope, functional group compatibility investigations,[18−20] testing of complex substrates (chemistry informers),[20,21] extensive reaction guidelines[22,23] and machine learning-based predictive models.[24,25] While these approaches provide valuable information on the scope of a particular methodology, we recognize the following limitations: (1) most studies focus on a single catalytic system, making cross-comparisons challenging; (2) complex substrate−catalyst interactions can unpredictably alter selectivity[26]; and (3) practical challenges, like low solubility or stability, often require independent testing. Experimental validation and optimization of LSF methods on the substrate

Received: December 13, 2024
Revised: January 23, 2025
Accepted: January 24, 2025
Published: February 12, 2025

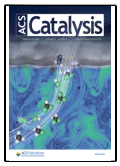

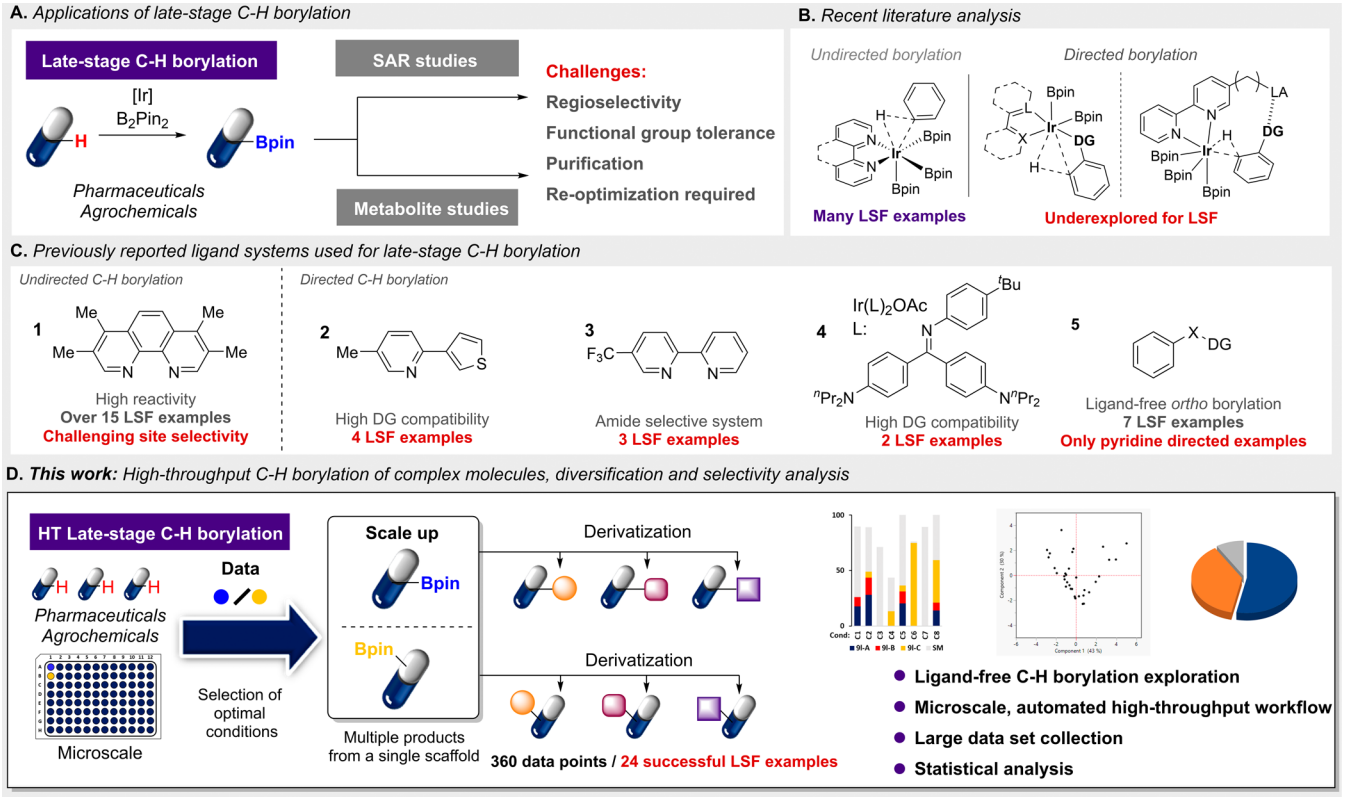

Figure 1. (A) Applications of late-stage C−H borylation. DG, directing group. (B) Undirected and directed C−H borylation. (C) Iridium catalyst and ligand structures with previous examples of LSF.[31,33,41,51,52] (D) High-throughput C−H borylation and diversification platform.

of interest thus remain of critical importance to their successful implementation.[27,28]

C−H borylation is an extraordinarily useful LSF method[10,29,30] thanks to the wide functional group tolerance[10,29−35] and the versatility of the organoboron intermediates in the context of structure−activity relationship studies and metabolite synthesis (Figure 1A).[33,36−41] Despite this utility, there are relatively few HTE studies focused specifically on LSF borylation, especially using functional group-directed C−H borylation strategies.[33,39] In contrast to the extensive ligand comparison studies available for C−C and C−N couplings,[21,42−44] C−H borylation catalysts are more often evaluated within a specific model substrate class. For example, many developed catalytic systems focus on the functionalization of small building blocks.[45−49] The lack of a direct comparison between methods makes it challenging to select a borylation system for a specific target, especially for substrates containing multiple directing groups, where selectivity and yield are often unpredictable. Recently, Nippa[25] has showcased the use of high-throughput techniques to investigate undirected LSF C−H borylation. This approach was further highlighted by Hartwig employing a bench stable iridium(I) cyclooctene complex to generate libraries of borylated compounds for subsequent derivatizations.[50] However, late-stage borylation using the functional group-directed approach has not seen equal attention (Figure 1B).[32,33]

Herein, we introduce an experimental HTE framework designed to rapidly assess the feasibility and positional selectivity of C−H borylation in complex substrates (Figure 1D). Our goal was to develop a rapid (2−3 days) assessment of all selectively accessible borylation positions with minimal starting material consumption (<20 mg) while generating high-quality reaction data. A wide array of mechanistically distinct methods is utilized in our screen, specifically emphasizing directed C−H borylation. The presented experimental setup formally fulfills the informer library definition[21] and allows us to draw important conclusions about the existing C−H borylation methods, their performance under high-throughput conditions, and the desirable future state of the field.

METHODS

Design of the C−H Borylation Panel. To create a screening platform for complex molecules (Figure 1D), we initially focused on selecting ligand and catalyst systems. The selected conditions should ideally afford different borylated products with complementary regioselectivity and tolerate various directing and spectator functional groups, ensuring complementary chemo-selectivity. The reaction conditions should be compatible with HTE; thus, reaction temperature significantly above the boiling point of the reaction solvent or apolar solvents with generally poor substrate solubility were excluded. Finally, we aimed to endorse diverse catalyst structures and mechanistic principles with a preference for protocols using commercially available or easily accessible ligands. After an extensive literature review, we selected the following five catalyst systems (Figure 1C).

1) $[Ir(COD)OMe]_2$/3,4,7,8-Tetramethyl-1,10-phenanthroline (**1**):[53−55] A prototypical example of the *N,N* ligand providing high activity for the undirected borylation of C−H bonds in arenes with regioselectivity controlled mostly by steric factors. For heterocyclic substrates,[23] anilines,[56] and phenols,[57] the electronic properties and

https://doi.org/10.1021/acscatal.4c07711
ACS Catal. 2025, 15, 3525−3534

other interactions can sometimes override the steric preferences.

2) $[Ir(COD)OMe]_2$/5-Methyl-2-(thiophen-3-yl)pyridine (**2**): A recently reported system for the directed borylation of aryl and heteroaryl C−H bonds compatible with various directing groups.[31]
3) $[Ir(COD)OMe]_2$/5-Trifluoromethyl-2,2′-bipyridine (**3**): Providing highly *ortho*-selective borylation of aromatic amides.[51]
4) A robust, single-component iridium(III) precatalyst (**4**) reported by our group for the borylation of aromatic, heteroaromatic, acrylic, and aliphatic systems.[52]
5) Ligand-free $[Ir(COD)OMe]_2$ catalyst: The simplest system, described for the *ortho*-selective borylation of substrates bearing heterocycle and benzylamine-derived directing groups.[41,58,59]

We then investigated whether the introduction of additives into our selected catalytic systems could expand the range of compatible substrates. Our initial focus was on HBpin as it has the potential to mask polar groups and alter regioselectivity.[56,60] Considering the previously reported catalyst activation and rate enhancement of **4**,[52] we included HBpin (1.0 equiv) as an additive with this catalyst system.

We found that under ligand-free conditions, the effect of HBpin can be either beneficial (heterocycle DG) or detrimental (amide DG) to the system depending on the substrate (Figure 2). We reasoned that for the amide **5a**

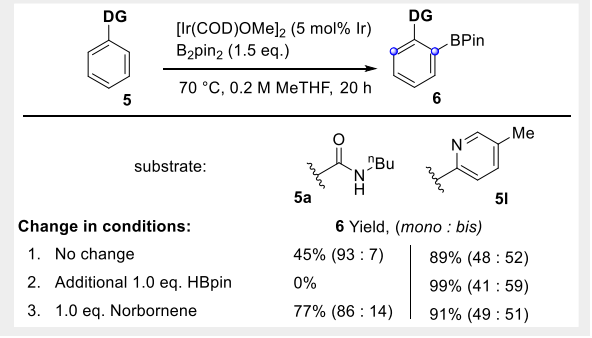

Figure 2. Optimization of ligand-free borylation.

potential side reactions with HBpin could cause a low yield, so we extensively screened potential HBpin scavengers (SI page 11) and found that norbornene (nbe) enhances product formation. These findings align with prior reports of nbe's advantageous role as a hydrogen acceptor in reactions involving silanes or boranes.[61−63]

Consequently, HBpin (1.0 equiv) was included as an additive with the precatalyst system **4** and nbe (1.0 equiv) or HBpin (1.0 equiv) with the ligand-free system. To minimize the number of reactions in our screen and thus the required substrate amount, we decided to omit solvent as a screening variable. We opted for MeTHF as the solvent of choice as it offers a balance of good solubilizing power for polar substrates and reagents, low reactivity, and a reasonably high boiling point along with improved sustainability since it is derived from lignocellulosic biomass. This gave a total number of eight screening conditions enabling the accommodation of up to 12 substrates on a 96-position screening plate.

Miniaturization Studies. Through miniaturization tests, we have demonstrated the ability to consistently maintain reactivity while reducing the reaction scale to 4 μmol and concentration to 0.04 M, provided that the reaction is conducted in a glovebox (refer to SI page 9). For an average substrate (M_w = 300), this equates to 9.6 mg for the eight conditions, which can be dispensed via solid dosing (Chronect Quantos) or preplated as a dimethylacetamide solution and then evaporated (using Genevac). For the distribution of catalysts, ligands, and additives, we chose to employ liquid handling of MeTHF stock solutions due to the superior distribution speed and accuracy. However, for the poorly soluble ligand **1**, chemical-coated glass beads (ChemBeads) were employed.[64]

C−H Borylation of Simple Molecules. With the reaction optimization module in hand, we embarked on validating our approach by borylating a series of increasingly complex aromatic and heteroaromatic fragments (Figure 3). The substrates **5** were deliberately selected not only to feature one potential directing group but also to contain functional groups typically present in lead-like compounds. Following the microscale screening of conditions C1−C8 (Figure 3A), selected conditions were replicated on a 0.5 mmol scale to isolate the products for structural determination and calibration of the screening yields (Figure 3B). Only products formed in high regioselectivity (>10:1) were isolated, as the separation of boronic esters can be quite challenging.[65−67] The HT screening results for each substrate across the eight methods are depicted using bar charts, which display the chemical yield of the regioisomers formed (in blue or yellow) as well as the remaining starting material (in gray) mass balance (Figure 3C).

Generally, the anticipated reactivity trends were observed with phenanthroline ligand **1** (condition C4) delivering the "undirected" borylation products, while the other conditions delivered the expected *ortho*-substituted products. The notable exception was substrate **6g**, where all conditions gave the same product; presumably, the electronic properties of the heterocycle override any directing effect of the amide group. Interestingly, significant differences in the performance of the various directed borylation methods were observed, highlighting the need to screen multiple conditions to find a suitable system for specific substrates. *Ortho*-borylated products **6a**, **6d**,[31] and **6f** could be obtained using the ligand-free conditions (C2, C3), which is particularly noteworthy as none of these substrate classes have been reported to undergo ligand-free borylation. Ligand-free conditions also proved most effective with a sulfonamide directing group (substrate **5j**), while conditions C4 selectively generated the other regioisomer. Conditions C5 and C6 appeared to be especially suitable for the thiomethyl directing group, yielding product **6c**. Conditions C6−C8 provided superior results for tertiary amides **6b**, **6e,** and **6i-A**. It is also worth noting that several conditions, including being ligand-free, were successful in providing the sp^3-borylated product **6h-A**. Overall, these results highlighted the versatility of the ligand-free conditions in combination with different additives; thus, we decided to keep all three variations for the complex molecule functionalization.

LSF and Diversification Studies. After formalizing and validating the reaction optimization setup using simple substrates, a series of commercially available pharmaceutical and agrochemical active ingredients were screened (Figures 4 and 5; see the SI for the full list of successful and unsuccessful substrates). This necessitated a change in our analytical

https://doi.org/10.1021/acscatal.4c07711
ACS Catal. 2025, 15, 3525−3534

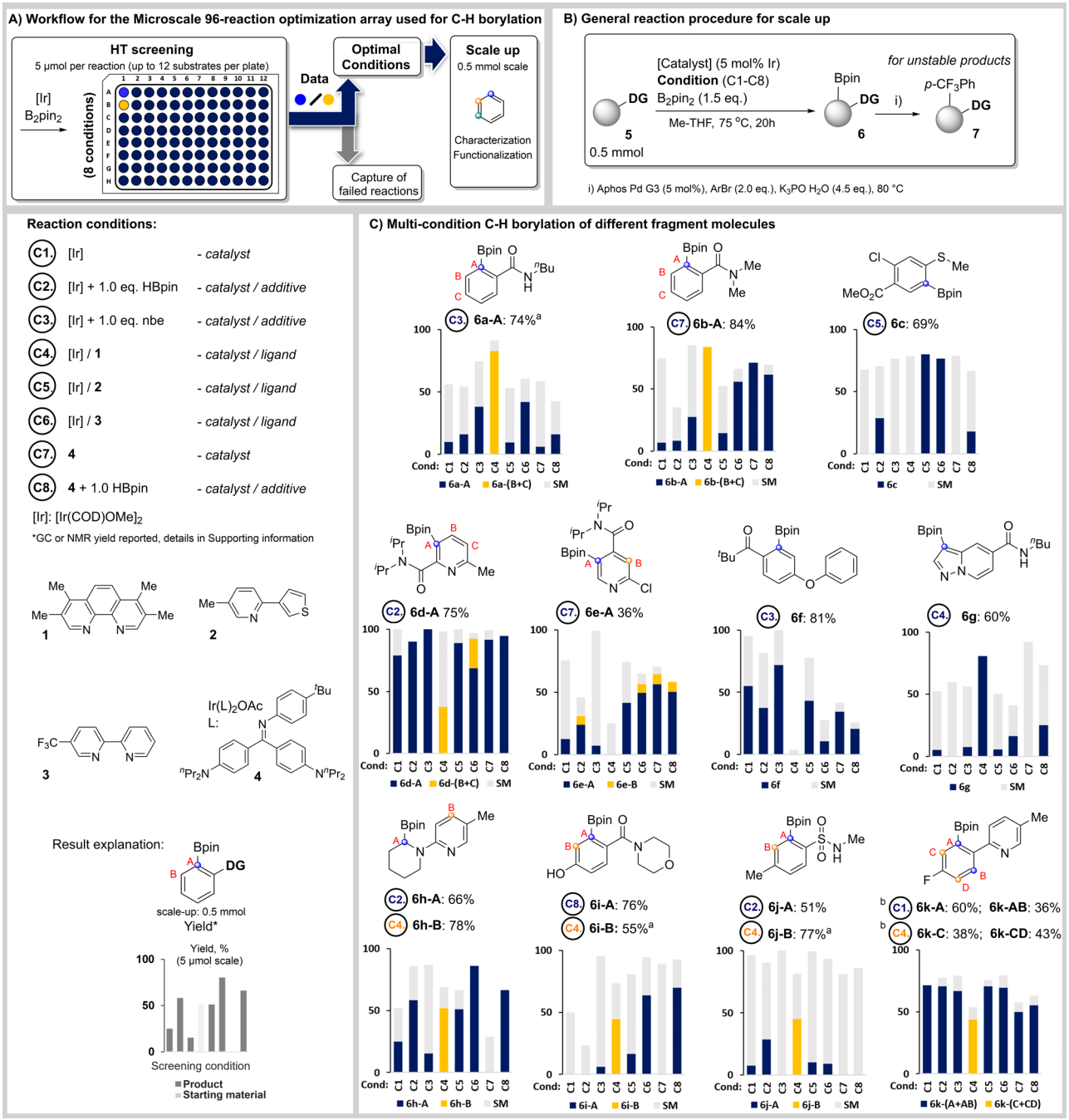

Figure 3. (A) Workflow for the Microscale 96-reaction optimization array used for C−H borylation chemistry evaluation. (B) General reaction procedure for scale-up. (C) Borylation of different fragment molecules. Reaction conditions C1−C8, reaction substrates **5a−k**, chemical yield of the regioisomers determined by calibrated GC or ^{1}H NMR. The isolated yield is generally lower due to product instability on silica; see the SI for details. [a]Combined yield of mono- and bis-product; see the SI for details. [b]Compound **6k** required subsequent Suzuki coupling of the reaction crude to isolate the products, and reported yields are prior to derivatization; see the SI for details.

workflow as most of the complex substrates were not suitable for analysis by GCMS. LCMS proved unreliable due to the variable stability of different boronates (hydrolysis, protodeborylation), and thus we turned to NMR analysis of the crude reaction mixtures. In general, it was possible to determine the ratio of regioisomers by inspection of the ^{1}H or ^{19}F spectra, and NMR has the advantage that direct quantification is possible using an internal standard without requiring a pure product sample for calibration. The conditions providing a single product in sufficient amount (>20%) were selected for scale-up, isolation, and structure elucidation of the product. Depending on the intermediate stability, the crude borylated products were either purified by silica chromatography, mass-guided SFC, or derivatized by Suzuki coupling or oxidation followed by preparative HPLC purification. Out of the 24 successful LSF examples reported, approximately half yielded a single isolated product (Figure 4). In the remaining cases, conditions with varying degrees of regioselectivity were identified, allowing the isolation of two or more regioisomeric products (Figure 5). Upon examination of the obtained products, it is evident that for numerous products (**11a−11e**, **10e**, **11k**, **11l-A**, **11m-A**, **9n-A**, **11r-A**, **9s-A**, **11t-A**), the *ortho*

https://doi.org/10.1021/acscatal.4c07711
ACS Catal. 2025, 15, 3525−3534

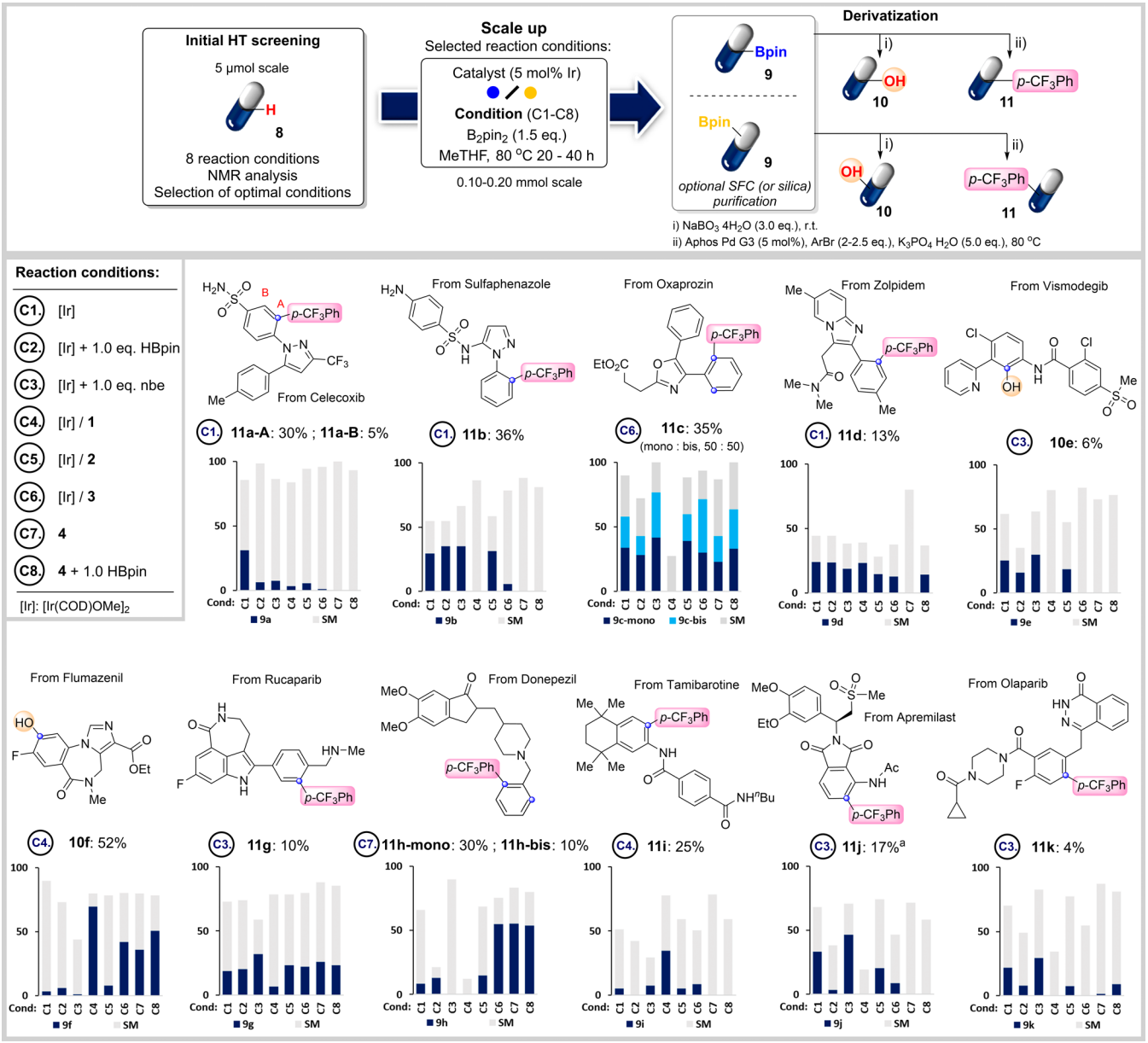

Figure 4. LSF of complex molecules via HT borylation screening. Isolated yields from reaction scale-up (using the specified reaction condition) reported underneath each structure; see the SI for details. [a]N−Ac group cleavage was observed during Suzuki coupling.

directing effect originates from an adjacent heterocycle, and the most favorable outcomes are generally observed under ligand-free conditions (C1−C3). Hydroxylated derivative **10e** has been previously identified as a product of Vismodegib metabolism in humans.[68]

Borylation of Diflufenican **8m** under ligand-free conditions has been reported previously, resulting in the same primary borylation isomer **9m-A** in 71% yield.[58] For Flumazenil (isolated product **10f**, borylation conditions C4), the regioselectivity appears to stem from the fluorine effect,[69] while in Rucaparib **11g** and Donepezil **11h**, benzylamine-directed borylation predominates.[41] *Ortho* borylation of amide and reverse amide functionalities has been achieved (**11i**, **11j**, **11m-B/C**, **11q-A**, **10w-A**, **11x-A/B**) under a variety of conditions, with the most productive being the ligand-free and nbe combination C3. Another major class of products originates from the *meta* borylation of the pyridine (**9n-B**, **10o**, **11p**, **11q-B**, and **10z**) and pyrazole (**9s-B**) heterocycles. The high activity of C6 in this respect is surprising as the regioselectivity of this ligand system has been primarily attributed to the presence of an amide directing group.[51] It is interesting to note that Cyprofuram delivered the *meta*-directed product **9y** under all of the working conditions C4−C8. While for condition C4, this can be explained by steric abstraction, it is noteworthy that conditions C5−C8 also delivered the same product.

Part of the mass balance loss could be attributed to the reduction of the starting material. For example, in the case of Parecoxib, under conditions C6, starting material reduction was observed as the major product, while for Apixaban, the major product results from simultaneous C−H functionalization and reduction (Figure 6). For Donepezil (**8h**) conditions, C2 seemed to reduce the carbonyl group. Interestingly, for Zolpidem **8d,** potential N-Me borylation was observed, but no corresponding product could be isolated, likely due to its

https://doi.org/10.1021/acscatal.4c07711
ACS Catal. 2025, 15, 3525−3534

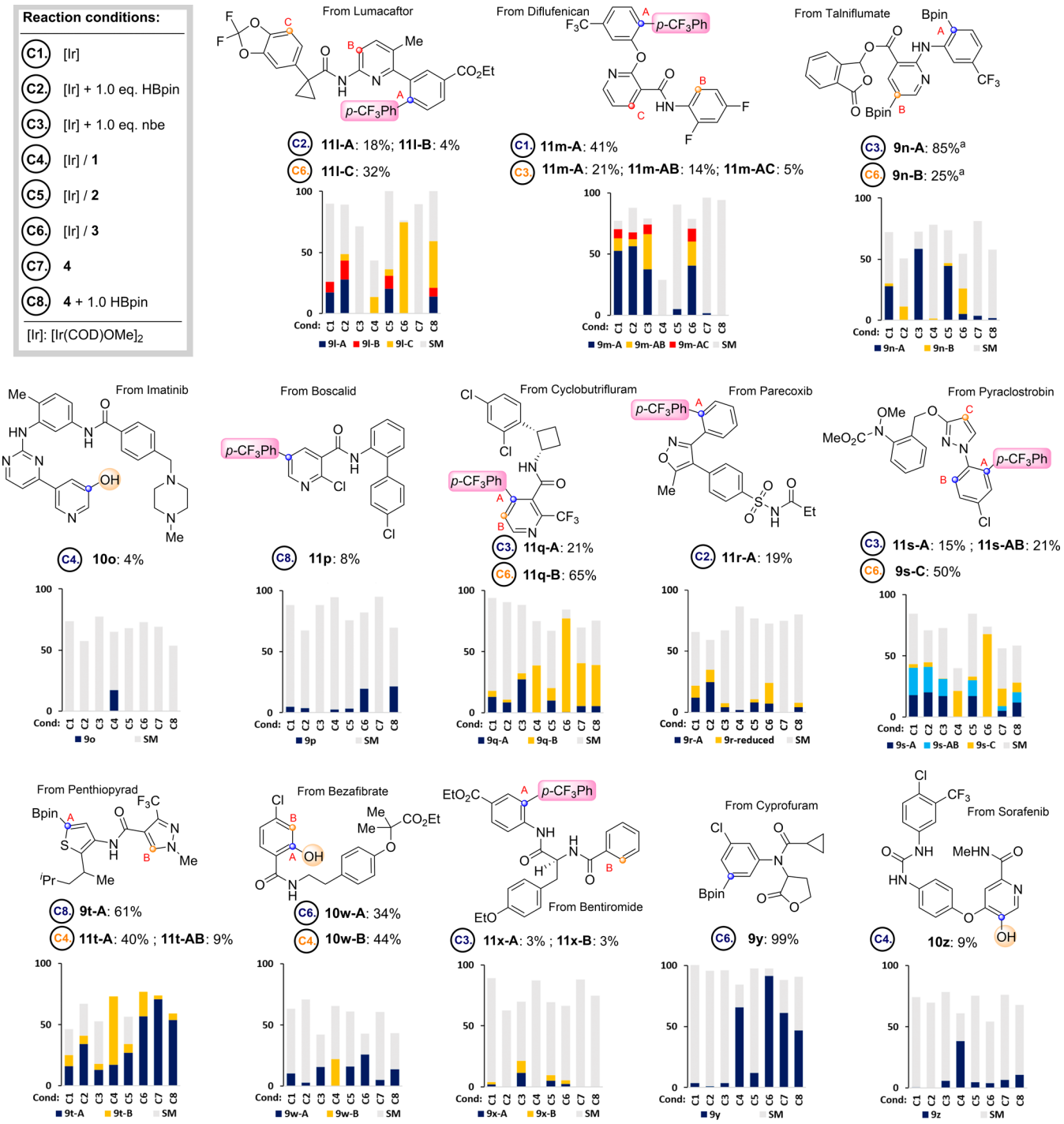

Figure 5. LSF of complex molecules via HT borylation screening. Isolated yields from reaction scale-up (using the specified reaction condition) reported under each structure; see the SI for details. [a]NMR yield, compound sensitive to purification, see the SI.

instability under Suzuki coupling conditions. This again highlights the complexity of applying C−H borylation to LSF.

Data Analysis. When developing a panel of LSF conditions such as this, throughput could be increased if the panel of conditions is reduced by identifying and eliminating "duplicate" reaction conditions. To this end, we analyzed the results of experiments **6a−k** and **9a−z** using a mixture of basic summary statistics and principal component analysis (PCA) to characterize the set of eight reaction conditions used in the panel.

The summary statistics (Figure 7) show that of the 45 screened complex molecules, 24 formed at least one borylated product that could be isolated (see the SI for the list of failed substrates). From the 24 successful LSF molecules, 14 produced a single product, while for 10, multiple products could be accessed. In total, 36 different products could be isolated, with an average isolated yield above 30%.

For PCA analysis, each individual product was recorded as a separate observation. This gave 21 unique products for the 11 simple and 36 products for the 24 complex substrates. For each borylation condition, average chemical yield, average ranking,

https://doi.org/10.1021/acscatal.4c07711
ACS Catal. 2025, 15, 3525−3534

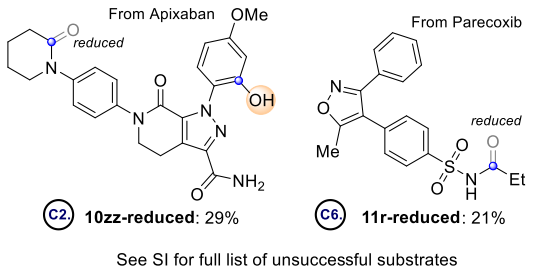

Figure 6. Isolated side-products from the LSF of complex molecules, details in the SI.

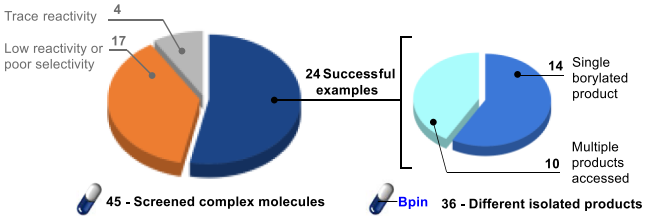

Figure 7. Statistical analysis of borylation products **9a–z** (LSF molecules).

and number of products obtained in at least 10% yield ("success rate") were calculated.

For the simple molecules **6a–k**, C6 was the best performer, giving more than a 10% yield for 11 out of 21 products. C8 gave similar results, with a very similar pattern of reactivity. The data were then reanalyzed with the 11 successful products removed to find out if there were conditions within the screen that could give orthogonal selectivity. Here, C4 was the best performer, giving more than 10% yield for eight of the remaining 10 products. The success of the C4 conditions was driven by its ability to produce the products that tended to be the minor products in most of the other conditions. The complementarity of the methods can be easily seen in the PCA plot (see the SI).

For complex molecules **9a–z**, C6 was again the best performer, giving at least 10% yield in 18 of 36 products. C8 in contrast ranked more toward the average, perhaps reflecting the catalyst's need for a clear site for coordination. The best orthogonal conditions here were the ligand-free C1 or C3, which gave at least 10% chemical yield in, respectively, 11 and 10 of the remaining 18 products. The PCA model (Figure 8) shows a pattern different from that of the simple molecules, with two groups of conditions emerging: C1/2/3/5 in the NW corner of the plot and C4/6/7/8 in the NE. This shows that

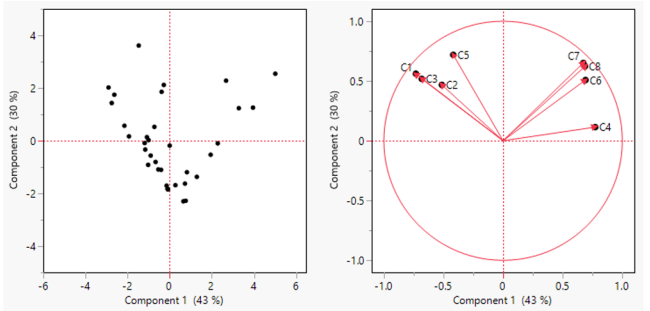

Figure 8. PCA analysis of the borylation product yields **9a–z** (LSF molecules).

the ligand-free conditions not only perform on par with the state-of-the-art ligand systems but also tend to provide unique reaction products, compared to the other tested conditions. Additionally, we found that the Mascarenas ligand **3** (C6), which should only work with amide directing groups, showed high reactivity and high *meta*-selectivity for numerous heterocycles.

The differences between the simple and complex system models, with their different patterns of catalyst performance, show how screening of multiple conditions can benefit LSF studies, as the site predictions based on the small molecules do not translate well in a complex molecule setting.

CONCLUSIONS

This study highlights the power of HTE as a practical tool to realize the potential of late-stage C–H borylation. An experimental workflow combining a microscale, multivariate reaction optimization and scale-up/derivatization was developed and shown to facilitate the efficient C–H borylation of a wide variety of fragments, drugs, and agrochemicals. The initial screen requires only a small amount of the substrate (~15 mg), and up to 12 molecules can be evaluated simultaneously, both significant advantages when working with valuable lead compounds under tight timelines (Figure 9).

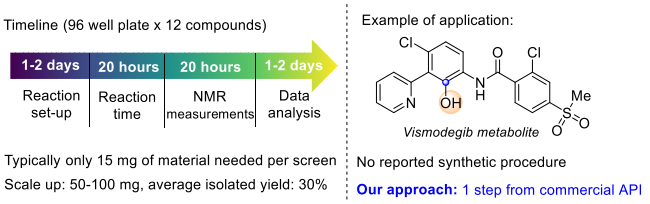

Figure 9. Timeline and application of the HTE borylation approach.

Using this platform, 24 structurally complex bioactive molecules were successfully derivatized, yielding 36 functionalized analogues in substantial quantities (median yield of 20 mg) and high purity, meeting the formal criteria for LSF.[11] The comprehensive reactivity data across a panel of eight state-of-the-art C–H borylation methods and an "informer library" of highly complex substrates revealed some surprising reactivity patterns.[21] Importantly, we have found that ligand-free borylation can often outperform other state-of-the-art borylation methods, and the introduction of additives (HBpin or nbe) can further improve this approach.[59] Additionally, ligands originally reported for *ortho*-directed borylation[31,51,52] may provide other useful regioselectivity outcomes. The obtained data set could be, in the future, used to enhance the predictive power of the existing computational models to include directed borylation.[24,25] The reported multicondition screening study could also stimulate a different thinking about what are the desirable attributes of a newly developed LSF methodology. In this context, high generality (e.g., a wide range of applicable directing groups) may not be the most crucial attribute of a method. Instead, a narrow specialization and complementarity to the existing methods may hold greater importance.

ASSOCIATED CONTENT

Supporting Information

The Supporting Information is available free of charge at https://pubs.acs.org/doi/10.1021/acscatal.4c07711.

https://doi.org/10.1021/acscatal.4c07711
ACS Catal. 2025, 15, 3525–3534

Experimental procedures, optimization of reaction conditions, characterization data, statistical data analysis, NMR spectra of novel compounds (PDF)

AUTHOR INFORMATION

Corresponding Author

Tomas Smejkal − *Research Chemistry, Syngenta Crop Protection AG, AG 4332 Stein, Switzerland;* orcid.org/0000-0001-9458-0963; Email: tomas.smejkal@syngenta.com

Authors

Janis M. Zakis − *Research Chemistry, Syngenta Crop Protection AG, AG 4332 Stein, Switzerland; Institut für Organische Chemie, Universität Würzburg, 97074 Würzburg, Germany*

Rebeka A. Lipina − *Research Chemistry, Syngenta Crop Protection AG, AG 4332 Stein, Switzerland*

Sharon Bell − *Research Chemistry, Syngenta Crop Protection AG, AG 4332 Stein, Switzerland*

Simon R. Williams − *Research Chemistry, Syngenta Crop Protection AG, AG 4332 Stein, Switzerland*

Maurus Mathis − *Research Chemistry, Syngenta Crop Protection AG, AG 4332 Stein, Switzerland*

Magnus J. Johansson − *Medicinal Chemistry, Research and Early Development, Cardiovascular, Renal and Metabolism (CVRM), BioPharmaceuticals R&D, AstraZeneca, 431 50 Gothenburg, Sweden;* orcid.org/0000-0002-0904-2835

Joanna Wencel-Delord − *Institut für Organische Chemie, Universität Würzburg, 97074 Würzburg, Germany*

Complete contact information is available at: https://pubs.acs.org/10.1021/acscatal.4c07711

Author Contributions

J.M.Z., M.J.J., J.W.-D., and T.S. conceived the project and designed the experiments. T.S. directed the project. J.M.Z., R.A.L, and M.M. performed and analyzed the experiments. S.B. performed the statistical analysis. J.M.Z, S.R.W., M.J.J., S.B., and T.S. reviewed and edited the manuscript.

Notes

The authors declare no competing financial interest.

ACKNOWLEDGMENTS

The authors thank Katharina Gaus and Thomas Stadelmann for NMR studies and structure elucidation, Sidney Behringer and Alexander Schuschkowski for preparative SFC purifications, Emma Jehle for preparative HPLC purifications, and Daria Grosheva and Julien Vantourout for fruitful discussions and help with revising the manuscript. The authors also thank AstraZeneca for providing the starting material for the LSF studies and the European Union H2020 research and innovation program under the Marie S. Curie Grant Agreement no. 860762 (MSCA ITN: CHAIR) and Syngenta Crop Protection AG for the extensive funding.

REFERENCES

(1) Shevlin, M. Practical High-Throughput Experimentation for Chemists. *ACS Med. Chem. Lett.* **2017**, *8* (6), 601−607.

(2) Krska, S. W.; DiRocco, D. A.; Dreher, S. D.; Shevlin, M. The Evolution of Chemical High-Throughput Experimentation To Address Challenging Problems in Pharmaceutical Synthesis. *Acc. Chem. Res.* **2017**, *50* (12), 2976−2985.

(3) Webb, E. W.; Cheng, K.; Winton, W. P.; Klein, B. J. C.; Bowden, G. D.; Horikawa, M.; Liu, S. W.; Wright, J. S.; Verhoog, S.; Kalyani, D.; et al. Development of High-Throughput Experimentation Approaches for Rapid Radiochemical Exploration. *J. Am. Chem. Soc.* **2024**, *146* (15), 10581−10590.

(4) Taylor, C. J.; Pomberger, A.; Felton, K. C.; Grainger, R.; Barecka, M.; Chamberlain, T. W.; Bourne, R. A.; Johnson, C. N.; Lapkin, A. A. A Brief Introduction to Chemical Reaction Optimization. *Chem. Rev.* **2023**, *123* (6), 3089−3126.

(5) Mennen, S. M.; Alhambra, C.; Allen, C. L.; Barberis, M.; Berritt, S.; Brandt, T. A.; Campbell, A. D.; Castañón, J.; Cherney, A. H.; Christensen, M.; et al. The Evolution of High-Throughput Experimentation in Pharmaceutical Development and Perspectives on the Future. *Org. Process Res. Dev.* **2019**, *23* (6), 1213−1242.

(6) Mahjour, B.; Zhang, R.; Shen, Y.; McGrath, A.; Zhao, R.; Mohamed, O. G.; Lin, Y.; Zhang, Z.; Douthwaite, J. L.; Tripathi, A.; et al. Rapid planning and analysis of high-throughput experiment arrays for reaction discovery. *Nat. Commun.* **2023**, *14* (1), 3924.

(7) Mahjour, B.; Shen, Y.; Cernak, T. Ultrahigh-Throughput Experimentation for Information-Rich Chemical Synthesis. *Acc. Chem. Res.* **2021**, *54* (10), 2337−2346.

(8) Shields, B. J.; Stevens, J.; Li, J.; Parasram, M.; Damani, F.; Alvarado, J. I. M.; Janey, J. M.; Adams, R. P.; Doyle, A. G. Bayesian reaction optimization as a tool for chemical synthesis. *Nature* **2021**, *590* (7844), 89−96.

(9) Cernak, T.; Dykstra, K. D.; Tyagarajan, S.; Vachal, P.; Krska, S. W. The medicinal chemist's toolbox for late stage functionalization of drug-like molecules. *Chem. Soc. Rev.* **2016**, *45* (3), 546−576.

(10) Guillemard, L.; Kaplaneris, N.; Ackermann, L.; Johansson, M. J. Late-stage C-H functionalization offers new opportunities in drug discovery. *Nat. Rev. Chem.* **2021**, *5* (8), 522−545.

(11) Zhang, L.; Ritter, T. A Perspective on Late-Stage Aromatic C-H Bond Functionalization. *J. Am. Chem. Soc.* **2022**, *144* (6), 2399−2414.

(12) Castellino, N. J.; Montgomery, A. P.; Danon, J. J.; Kassiou, M. Late-stage Functionalization for Improving Drug-like Molecular Properties. *Chem. Rev.* **2023**, *123* (13), 8127−8153.

(13) Genovino, J.; Sames, D.; Hamann, L. G.; Toure, B. B. Accessing Drug Metabolites via Transition-Metal Catalyzed C-H Oxidation: The Liver as Synthetic Inspiration. *Angew. Chem., Int. Ed.* **2016**, *55* (46), 14218−14238.

(14) Antermite, D.; Friis, S. D.; Johansson, J. R.; Putra, O. D.; Ackermann, L.; Johansson, M. J. Late-stage synthesis of heterobifunctional molecules for PROTAC applications via ruthenium-catalysed C−H amidation. *Nat. Commun.* **2023**, *14* (1), 8222.

(15) Brown, D. G.; Bostrom, J. Analysis of Past and Present Synthetic Methodologies on Medicinal Chemistry: Where Have All the New Reactions Gone? *J. Med. Chem.* **2016**, *59* (10), 4443−4458.

(16) Dombrowski, A. W.; Aguirre, A. L.; Shrestha, A.; Sarris, K. A.; Wang, Y. The Chosen Few: Parallel Library Reaction Methodologies for Drug Discovery. *J. Org. Chem.* **2022**, *87* (4), 1880−1897.

(17) Wang, Y.; Haight, I.; Gupta, R.; Vasudevan, A. What is in Our Kit? An Analysis of Building Blocks Used in Medicinal Chemistry Parallel Libraries. *J. Med. Chem.* **2021**, *64* (23), 17115−17122.

(18) Collins, K. D.; Glorius, F. A robustness screen for the rapid assessment of chemical reactions. *Nat. Chem.* **2013**, *5* (7), 597−601.

(19) Gensch, T.; Glorius, F. The straight dope on the scope of chemical reactions. *Science* **2016**, *352* (6283), 294−295.

(20) Friis, S. D.; Johansson, M. J.; Ackermann, L. Cobalt-catalysed C-H methylation for late-stage drug diversification. *Nat. Chem.* **2020**, *12* (6), 511−519.

(21) Kutchukian, P. S.; Dropinski, J. F.; Dykstra, K. D.; Li, B.; DiRocco, D. A.; Streckfuss, E. C.; Campeau, L. C.; Cernak, T.; Vachal, P.; Davies, I. W.; et al. Chemistry informer libraries: a chemoinformatics enabled approach to evaluate and advance synthetic methods. *Chem. Sci.* **2016**, *7* (4), 2604−2613.

(22) Weis, E.; Johansson, M.; Korsgren, P.; Martin-Matute, B.; Johansson, M. J. Merging Directed C-H Activations with High-Throughput Experimentation: Development of Iridium-Catalyzed C-

H Aminations Applicable to Late-Stage Functionalization. *JACS Au* **2022**, *2* (4), 906−916.
(23) Larsen, M. A.; Hartwig, J. F. Iridium-catalyzed C-H borylation of heteroarenes: scope, regioselectivity, application to late-stage functionalization, and mechanism. *J. Am. Chem. Soc.* **2014**, *136* (11), 4287−4299.
(24) Caldeweyher, E.; Elkin, M.; Gheibi, G.; Johansson, M.; Skold, C.; Norrby, P. O.; Hartwig, J. F. Hybrid Machine Learning Approach to Predict the Site Selectivity of Iridium-Catalyzed Arene Borylation. *J. Am. Chem. Soc.* **2023**, *145* (31), 17367−17376.
(25) Nippa, D. F.; Atz, K.; Hohler, R.; Muller, A. T.; Marx, A.; Bartelmus, C.; Wuitschik, G.; Marzuoli, I.; Jost, V.; Wolfard, J.; et al. Enabling late-stage drug diversification by high-throughput experimentation with geometric deep learning. *Nat. Chem.* **2024**, *16* (2), 239−248.
(26) Zakis, J. M.; Smejkal, T.; Wencel-Delord, J. Cyclometallated complexes as catalysts for C-H activation and functionalization. *Chem. Commun.* **2022**, *58* (4), 483−490.
(27) Krska, S. W.; Li, B.; Tyagarajan, S.; Dykstra, K. D.; Cernak, T.; Vachal, P. Harnessing the Power of C−H Functionalization Chemistry to Accelerate Drug Discovery. *Synlett* **2024**, *35* (08), 862−876.
(28) Friis, S. D.; Weis, E.; Johansson, M. J. *The Power of High-Throughput Experimentation: Case Studies from Drug Discovery, Drug Development, and Catalyst Discovery (Volume 2) (ACS Symposium Series)*; ACS Publications, 2022, *1420*, 161−179.
(29) Ishiyama, T.; Takagi, J.; Ishida, K.; Miyaura, N.; Anastasi, N. R.; Hartwig, J. F. Mild iridium-catalyzed borylation of arenes. High turnover numbers, room temperature reactions, and isolation of a potential intermediate. *J. Am. Chem. Soc.* **2002**, *124* (3), 390−391.
(30) Smith, M. R., 3rd; Bisht, R.; Haldar, C.; Pandey, G.; Dannatt, J. E.; Ghaffari, B.; Maleczka, R. E., 3rd; Chattopadhyay, B. Achieving High Ortho Selectivity in Aniline C-H Borylations by Modifying Boron Substituents. *ACS Catal.* **2018**, *8* (7), 6216−6223.
(31) Hoque, M. E.; Hassan, M. M. M.; Chattopadhyay, B. Remarkably Efficient Iridium Catalysts for Directed C(sp(2))-H and C(sp(3))-H Borylation of Diverse Classes of Substrates. *J. Am. Chem. Soc.* **2021**, *143* (13), 5022−5037.
(32) Hassan, M. M. M.; Guria, S.; Dey, S.; Das, J.; Chattopadhyay, B. Transition metal-catalyzed remote C-H borylation: An emerging synthetic tool. *Sci. Adv.* **2023**, *9* (16), No. eadg3311.
(33) Yu, I. F.; Wilson, J. W.; Hartwig, J. F. Transition-Metal-Catalyzed Silylation and Borylation of C-H Bonds for the Synthesis and Functionalization of Complex Molecules. *Chem. Rev.* **2023**, *123* (19), 11619−11663.
(34) Oeschger, R.; Su, B.; Yu, I.; Ehinger, C.; Romero, E.; He, S.; Hartwig, J. Diverse functionalization of strong alkyl C-H bonds by undirected borylation. *Science* **2020**, *368* (6492), 736−741.
(35) Hartwig, J. F.; Larsen, M. A. Undirected, Homogeneous C-H Bond Functionalization: Challenges and Opportunities. *ACS Cent. Sci.* **2016**, *2* (5), 281−292.
(36) West, M. J.; Fyfe, J. W. B.; Vantourout, J. C.; Watson, A. J. B. Mechanistic Development and Recent Applications of the Chan-Lam Amination. *Chem. Rev.* **2019**, *119* (24), 12491−12523.
(37) Mkhalid, I. A.; Barnard, J. H.; Marder, T. B.; Murphy, J. M.; Hartwig, J. F. C-H activation for the construction of C-B bonds. *Chem. Rev.* **2010**, *110* (2), 890−931.
(38) Darses, S.; Genet, J. P. Potassium organotrifluoroborates: new perspectives in organic synthesis. *Chem. Rev.* **2008**, *108* (1), 288−325.
(39) Saito, Y.; Yamanoue, K.; Segawa, Y.; Itami, K. Selective Transformation of Strychnine and 1,2-Disubstituted Benzenes by C−H Borylation. *Chem.* **2020**, *6* (4), 985−993.
(40) Partridge, B. M.; Hartwig, J. F. Sterically controlled iodination of arenes via iridium-catalyzed C-H borylation. *Org. Lett.* **2013**, *15* (1), 140−143.
(41) Scott, J. S.; Moss, T. A.; Barlaam, B.; Davey, P. R. J.; Fairley, G.; Gangl, E. T.; Greenwood, R. D. R.; Hatoum-Mokdad, H.; Lister, A. S.; Longmire, D.; et al. Addition of Fluorine and a Late-Stage Functionalization (LSF) of the Oral SERD AZD9833. *ACS Med. Chem. Lett.* **2020**, *11* (12), 2519−2525.
(42) Martin, R.; Buchwald, S. L. Palladium-catalyzed Suzuki-Miyaura cross-coupling reactions employing dialkylbiaryl phosphine ligands. *Acc. Chem. Res.* **2008**, *41* (11), 1461−1473.
(43) Lo, Q. A.; Sale, D.; Braddock, D. C.; Davies, R. P. Mechanistic and Performance Studies on the Ligand-Promoted Ullmann Amination Reaction. *ACS Catal.* **2018**, *8* (1), 101−109.
(44) Gensch, T.; Smith, S. R.; Colacot, T. J.; Timsina, Y. N.; Xu, G.; Glasspoole, B. W.; Sigman, M. S. Design and Application of a Screening Set for Monophosphine Ligands in Cross-Coupling. *ACS Catal.* **2022**, *12* (13), 7773−7780.
(45) Seechurn, C. C. C. J.; Sivakumar, V.; Satoskar, D.; Colacot, T. J. Iridium-Catalyzed C−H Borylation of Heterocycles Using an Overlooked 1,10-Phenanthroline Ligand: Reinventing the Catalytic Activity by Understanding the Solvent-Assisted Neutral to Cationic Switch. *Organometallics* **2014**, *33* (13), 3514−3522.
(46) Slack, E. D.; Colacot, T. J. Understanding the Activation of Air-Stable Ir(COD)(Phen)Cl Precatalyst for C-H Borylation of Aromatics and Heteroaromatics. *Org. Lett.* **2021**, *23* (5), 1561−1565.
(47) Peruzzi, C. D.; Miller, S. L.; Dannatt, J. E.; Ghaffari, B.; Maleczka, R. E., Jr.; Smith, M. R., 3rd A Hydrazone Ligand for Iridium-Catalyzed C-H Borylation: Enhanced Reactivity and Selectivity for Fluorinated Arenes. *Organometallics* **2024**, *43* (11), 1208−1212.
(48) Li, C. Y.; Zhang, Z.; Yan, X. Ir-Catalyzed Ortho-Selective C-H Borylation of Difluoromethyl Arenes. *Org. Lett.* **2023**, *25* (40), 7278−7282.
(49) Ghaffari, B.; Preshlock, S. M.; Plattner, D. L.; Staples, R. J.; Maligres, P. E.; Krska, S. W.; Maleczka, R. E., Jr.; Smith, M. R., 3rd Silyl phosphorus and nitrogen donor chelates for homogeneous ortho borylation catalysis. *J. Am. Chem. Soc.* **2014**, *136* (41), 14345−14348.
(50) D'Angelo, K. A.; La, C.; Kotecki, B.; Wilson, J. W.; Karmel, C.; Swiatowiec, R.; Tu, N. P.; Shekhar, S.; Hartwig, J. F. An Air-Stable, Single-Component Iridium Precatalyst for the Borylation of C-H Bonds on Large to Miniaturized Scales. *J. Am. Chem. Soc.* **2024**, *146* (47), 32717−32729.
(51) Marcos-Atanes, D.; Vidal, C.; Navo, C. D.; Peccati, F.; Jimenez-Oses, G.; Mascarenas, J. L. Iridium-Catalyzed ortho-Selective Borylation of Aromatic Amides Enabled by 5-Trifluoromethylated Bipyridine Ligands. *Angew. Chem., Int. Ed.* **2023**, *62* (18), No. e202214510.
(52) Zakis, J. M.; Messinis, A. M.; Ackermann, L.; Smejkal, T.; Wencel-Delord, J. Air-Stable Bis-Cyclometallated Iridium Catalysts for Ortho-Directed C(sp2)−H Borylation. *Adv. Synth. Catal.* **2024**, *366* (10), 2292−2304.
(53) Boller, T. M.; Murphy, J. M.; Hapke, M.; Ishiyama, T.; Miyaura, N.; Hartwig, J. F. Mechanism of the mild functionalization of arenes by diboron reagents catalyzed by iridium complexes. Intermediacy and chemistry of bipyridine-ligated iridium trisboryl complexes. *J. Am. Chem. Soc.* **2005**, *127* (41), 14263−14278.
(54) Preshlock, S. M.; Ghaffari, B.; Maligres, P. E.; Krska, S. W.; Maleczka, R. E., Jr.; Smith, M. R., 3rd High-throughput optimization of Ir-catalyzed C-H borylation: a tutorial for practical applications. *J. Am. Chem. Soc.* **2013**, *135* (20), 7572−7582.
(55) Oeschger, R. J.; Larsen, M. A.; Bismuto, A.; Hartwig, J. F. Origin of the Difference in Reactivity between Ir Catalysts for the Borylation of C-H Bonds. *J. Am. Chem. Soc.* **2019**, *141* (41), 16479−16485.
(56) Preshlock, S. M.; Plattner, D. L.; Maligres, P. E.; Krska, S. W.; Maleczka, R. E., Jr.; Smith, M. R., 3rd A traceless directing group for C-H borylation. *Angew. Chem., Int. Ed.* **2013**, *52* (49), 12915−12919.
(57) Chattopadhyay, B.; Dannatt, J. E.; Andujar-De Sanctis, I. L.; Gore, K. A.; Maleczka, R. E., Jr.; Singleton, D. A.; Smith, M. R., 3rd. Ir-Catalyzed ortho-Borylation of Phenols Directed by Substrate-Ligand Electrostatic Interactions: A Combined Experimental/in Silico Strategy for Optimizing Weak Interactions. *J. Am. Chem. Soc.* **2017**, *139* (23), 7864−7871.

https://doi.org/10.1021/acscatal.4c07711
ACS Catal. 2025, 15, 3525−3534

(58) Mahamudul Hassan, M. M.; Mondal, B.; Singh, S.; Haldar, C.; Chaturvedi, J.; Bisht, R.; Sunoj, R. B.; Chattopadhyay, B. Ir-Catalyzed Ligand-Free Directed C-H Borylation of Arenes and Pharmaceuticals: Detailed Mechanistic Understanding. *J. Org. Chem.* **2022**, *87* (6), 4360−4375.
(59) Zakis, J. M.; Kuhn, S. L.; Wencel-Delord, J.; Smejkal, T. Do we really need ligands in Ir-catalyzed C-H borylation? *Chimia* **2024**, *78* (7−8), 513−517.
(60) Le, N.; Chuang, N. L.; Oliver, C. M.; Samoshin, A. V.; Hemphill, J. T.; Morris, K. C.; Hyland, S. N.; Guan, H.; Webster, C. E.; Clark, T. B. Hidden Role of Borane in Directed C−H Borylation: Rate Enhancement through Autocatalysis. *ACS Catal.* **2023**, *13* (19), 12877−12893.
(61) Sasaki, I.; Amou, T.; Ito, H.; Ishiyama, T. Iridium-catalyzed ortho-C-H borylation of aromatic aldimines derived from pentafluoroaniline with bis(pinacolate)diboron. *Org. Biomol. Chem.* **2014**, *12* (13), 2041−2044.
(62) Wilson, J. W.; Su, B.; Yoritate, M.; Shi, J. X.; Hartwig, J. F. Iridium-Catalyzed, Site-Selective Silylation of Secondary C(sp(3))-H Bonds in Secondary Alcohols and Ketones. *J. Am. Chem. Soc.* **2023**, *145* (36), 19490−19495.
(63) Teo, W. J.; Yang, X.; Poon, Y. Y.; Ge, S. Cobalt-catalyzed deoxygenative triborylation of allylic ethers to access 1,1,3-triborylalkanes. *Nat. Commun.* **2020**, *11* (1), 5193.
(64) Impastato, A. C.; Brown, J. T. C.; Wang, Y.; Tu, N. P. Readily Accessible High-Throughput Experimentation: A General Protocol for the Preparation of ChemBeads and EnzyBeads. *ACS Med. Chem. Lett.* **2023**, *14* (4), 514−520.
(65) Wright, J. S.; Scott, P. J. H.; Steel, P. G. Iridium-Catalysed C-H Borylation of Heteroarenes: Balancing Steric and Electronic Regiocontrol. *Angew. Chem., Int. Ed.* **2021**, *60* (6), 2796−2821.
(66) Oka, N.; Yamada, T.; Sajiki, H.; Akai, S.; Ikawa, T. Aryl Boronic Esters Are Stable on Silica Gel and Reactive under Suzuki-Miyaura Coupling Conditions. *Org. Lett.* **2022**, *24* (19), 3510−3514.
(67) Hayes, H. L. D.; Wei, R.; Assante, M.; Geogheghan, K. J.; Jin, N.; Tomasi, S.; Noonan, G.; Leach, A. G.; Lloyd-Jones, G. C. Protodeboronation of (Hetero)Arylboronic Esters: Direct versus Prehydrolytic Pathways and Self-/Auto-Catalysis. *J. Am. Chem. Soc.* **2021**, *143* (36), 14814−14826.
(68) Graham, R. A.; Lum, B. L.; Morrison, G.; Chang, I.; Jorga, K.; Dean, B.; Shin, Y. G.; Yue, Q.; Mulder, T.; Malhi, V.; et al. A single dose mass balance study of the Hedgehog pathway inhibitor vismodegib (GDC-0449) in humans using accelerator mass spectrometry. *Drug. Metab. Dispos.* **2011**, *39* (8), 1460−1467.
(69) Pabst, T. P.; Chirik, P. J. A Tutorial on Selectivity Determination in C(sp(2))-H Oxidative Addition of Arenes by Transition Metal Complexes. *Organometallics* **2021**, *40* (7), 813−831.

https://doi.org/10.1021/acscatal.4c07711
ACS Catal. 2025, 15, 3525−3534